

Preparation and characterization of mesostructured polymer-functionalized sol–gel-derived thin films

B. Smarsly^a, G. Garnweitner^a, R. Assink^b, C. Jeffrey Brinker^{a,b,*}

^a University of New Mexico, Center for Micro-Engineered Materials, Advanced Materials Laboratory,
1001 University Blvd. SE, Albuquerque, NM 87106, USA

^b Sandia National Laboratories, MS 1349, Albuquerque, NM 87185, USA

Abstract

The present study attempts to incorporate methacrylate-based polymers into ordered lamellar organic/inorganic nanocomposite films composed of alternating SiO₂/polymer layers. The films are prepared by dip-coating from a solution containing the monomers and silica precursors, thus leading to composite lamellar mesostructured materials through evaporation-induced self-assembly (EISA). A polymerizable coupling agent is added to covalently link the polymers to the silica matrix. The final polymer/SiO₂ hybrid material is obtained by a separate free-radical polymerization step, initiated by UV exposure or thermal treatment. Using trimethoxy(7-octen-1-yl)silane as a coupling agent, a procedure was established that preserved the mesostructure and maintained the swelling properties of the polymers, while acrylate-based coupling agents lead to a significant distortion of the film mesostructure. Structure and composition of the films were studied by X-ray diffraction, NMR and IR.

© 2003 Published by Elsevier B.V.

Keywords: Sol–gel; Nanocomposite thin films; Free-radical polymerization; Hydrogel nanocomposites

1. Introduction

The preparation of surfactant-templated silica thin films, possessing various types of nanoscopic mesostructures such as 2D hexagonal cylinders or 3D hexagonal and cubic lattices, via sol–gel processing, has attained great attention in the past years because of potential applications as sensors, optoelectronic devices, etc., and also partly due to straightforward coating preparation methods [1–5]. As the key step, sol–gel chemistry is combined with the texture imposed by surfactant-mediated evaporation-induced self-assembly (EISA) [2]. Typically, a substrate is dip-coated or spin-coated with an acidic aqueous solution of a structure-directing surfactant such as CTAB (cetyltrimethylammonium bromide), a silica precursor such as TEOS (tetraethyl orthosilicate) and a water-miscible, volatile solvent (e.g. ethanol). The surfactant concentration increases upon evaporation of the solvent, and at a certain concentration co-self-assembly of the surfactant and silica species occurs, finally leading to self-assembled organized structures such as lamellae, cylindrical rods, etc. Recent publications indicate that the final mesostructure is a function of various parameters such as the CTAB/TEOS ratio, pH value, the evaporation rate, humidity, etc. [6–11].

Thin films with well-defined 2D and 3D mesostructured porosity are accessible via the EISA process by removing the structure-directing agent by extraction or calcination [6–11]. One of the most promising applications of these mesoscopically ordered silica films is their use as insulators in integrated circuit devices due to their low dielectric constant [12].

Aside from the preparation of mesoporous silica thin films, the incorporation of functional organic moieties into the mesostructure by EISA has attracted a great deal of attention. The underlying idea is to combine interesting optical, electro-optical or thermal properties of organic materials with the features of an inorganic silica framework. By this approach, the functionality of the relatively fragile organic moiety can be mediated through the rigid inorganic framework, providing both protection and also the 2D or 3D platform for the alignment and attachment of the organic matter. Various recent publications describe the preparation of inorganic/polymer hybrid coatings, mostly using silica as the inorganic part [13–16]. For example, the hardness of conducting polymer coatings was drastically increased by preparing a composite film, using sol–gel processing [16]. Also, titania-based high-refractive-index thin films have been obtained through sol–gel processing, however not possessing mesoscale order. Recently, several strategies have been reported by our group on the preparation

* Corresponding author. Tel.: +1-505-272-7627; fax: +1-505-272-7336.
E-mail address: cjbrink@sandia.gov (C.J. Brinker).

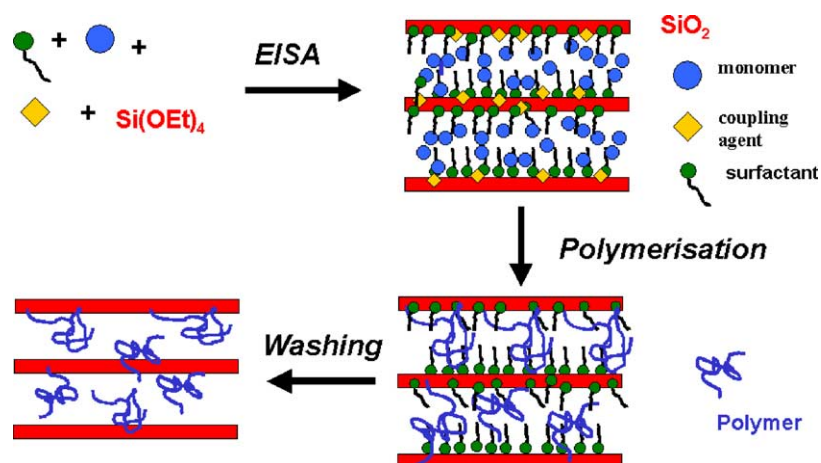


Fig. 1. Schematic representation of the incorporation of polymers in a siliceous nanocomposite by the EISA procedure, as used in this study. The initiator is omitted.

of mesostructured organic/inorganic nanocomposites using two different pathways to place an organic moiety tightly fixed into the inorganic framework of a mesostructured film. The organic compound is either covalently linked to a silica precursor prior to film preparation [17], or embedded between the siliceous walls during the self-assembly [18]. In the present study, we followed the second route and attempted to incorporate acrylate/amide-based polymers with interesting physico-chemical properties into a nanocomposite, prepared by the EISA process. The general procedure is illustrated in Fig. 1. As previous studies have shown, siliceous poly(diacetylene) nanocomposite films can be rapidly formed using polymerizable amphiphilic diacetylene monomers as both structure-directing agents and monomers [19]. In a further work, poly(dodecyl methacrylate) was successfully integrated into a thin silica film with a lamellar mesostructure [18]. In both cases, it turned out that adding monomers to the feed solution and conducting a free-radical polymerization procedure after the EISA process represents a promising pathway. However, the incorporation of polymers into nanostructured films still represents a challenge for materials scientists:

1. In general, polymers undergo substantial changes in their hydrophobic/hydrophilic behavior compared to the monomers, which may eventually lead to phase separation after polymerization and can cause damage to the mesostructure. Adding monomers and initiators may impair the self-assembly and aggravate the structure formation.
2. In a classical free-radical polymerization, the degree of polymerization and the amount of cross-linking strongly depend on various parameters such as the chosen initiator, the initiator concentration, etc. The optimum synthesis conditions for thin films may be different from bulk systems.
3. Self-assembly processes are characterized by a fine interfacial balance between hydrophilic and hydrophobic

moieties. In this study, coupling agents (equipped with a polymerizable double bond as well as an alkoxy group) were used to link the polymer to the siliceous matrix. This coupling could lead to a distortion of the mesostructure.

The objective of the work reported here is manifold. First, using the poly(dodecyl methacrylate) system mentioned above [18], the structureforming and polymerization processes are studied in detail by X-ray scattering (XRD) and IR/NMR. Second, the polymerization of acrylates is studied by a variation of the polymerization conditions, such as UV exposure and temperature treatment. Finally, it is attempted to copolymerize the methacrylate with *N*-isopropylacrylamide (NIPAAM) within the nanocomposite. PNIPAAM shows great promise because of its thermoresponsive behavior in an aqueous environment [20,21], which is maintained in copolymers with poly(methacrylates) [22]. It has been recently reported that PNIPAAM can be incorporated into a claycomposite, however this was accompanied by a significant loss in the mesostructured ordering [23]. XRD is used to monitor the structural changes during the various preparation steps to study the swelling behavior.

2. Experimental

Solution assembly. Precursor solutions were prepared using an acidic silica sol (A2**) made by mixing and heating TEOS (tetraethyl orthosilicate), ethanol (EtOH), deionized water and dilute HCl (molar ratios 1:3.8:1:5 × 10⁻⁵) to 60 °C and stirring for 90 min. Additional ethanol or another organic solvent, water and dilute hydrochloric acid (0.07 N) were subsequently inserted into the sol. Then a coupling agent was added, followed by the structure-directing agent (cetyltrimethylammonium bromide, CTAB). Various silanes such as trimethoxy(7-octen-1-yl)silane (7-OTS), 3-(trimethoxysilyl)propyl acrylate (PATMS) and 3-(trimethoxysilyl)propyl methacrylate (MPS) were used

as coupling agents to provide a link between the polymer phase and the silica framework. After dissolution of CTAB, the organic monomers (dodecyl methacrylate and/or *N*-isopropylacrylamide) were added, followed by a photosensitive initiator (benzoin dimethylether, BME) or a thermal initiator (1,1'-azobis(1-cyclohexanecarbonitrile), ACHN). The standard molar ratio of reactants in the final solution was 1 TEOS:22 EtOH:5 H₂O:0.004 HCl:0.21 CTAB:0.16 coupling agent:0.32–0.46 organic monomer:0.02–0.04 initiator. The solution was homogenized in an ultrasonic bath for 5 min. Finally, it was filtered through a Gelman Acrodisc PTFE 0.2 μm pore size filter.

Film preparation. (100)-silicon wafers were cleaned by washing with acetone and then calcined at 450 °C for 6 h. This pre-treatment led to a less hydrophilic surface that caused less de-wetting of the newly prepared films. Dust was removed by spraying the wafers with compressed N₂, and dip-coating was performed in a glove box under dry nitrogen (relative humidity of 2%). The standard dip-coating speed was 50.9 cm min⁻¹. After drying for about 10 min, the wafers were either irradiated with UV light of 365 nm for 2 h (using a UVP UVLM-26 6 W Hg arc lamp source with filter) or heat-treated in an oven at 120 °C for 3 h. To increase the siloxane condensation, the photo-initiated samples were exposed to ammonia vapor for 15–20 min after polymerization. This seemed to be most effective using a closed jar and concentrated ammonia (30% solution in water). To remove the surfactant and any remaining monomers, the samples then were subsequently washed with ethanol and acetone. A larger amount of material needed for IR and NMR measurements was obtained by applying a few drops of the solution onto a Petri dish placed in an upright position to get a thin layer by vertical draining. The polymerization was carried out as described above.

Characterization. The films were analyzed by X-ray diffraction (XRD), using a Siemens D500 diffractometer featuring Cu Kα radiation filtered with Ni (λ = 1.5418 Å). The typical 2θ range used was 1.2–10.0°. Samples for IR

measurements were prepared by scraping the dried film off the Petri dish, mixing it with potassium bromide (KBr) and then pressing it to get a clear pellet. A Bruker Vector22 Fourier-transform infrared (FTIR) spectrometer was used to obtain the IR spectra. Solid-state ¹³C magic-angle spinning (MAS) NMR measurements were performed on a 400 MHz Bruker AMX spectrometer using films scraped off a Petri dish. The ¹³C experiments were performed at 100.6 MHz using direct polarization and high-powered ¹H decoupling, with a delay time of 8 s and 1024 scans; the samples were spun at 12 kHz in a 4 mm MAS probe. Several different delay times were used for each sample in order to ensure that the recorded spectra were essentially quantitative. In order to investigate the optimum UV irradiation wavelength for photo-initiation, UV spectra were recorded using a Perkin-Elmer Lambda 45 spectrometer. Solutions of BME and NIPAAM in ethanol were measured (data not shown). The BME spectra feature a small absorbance maximum around 330–355 nm, and a strong peak at 250 nm. NIPAAM absorbs UV irradiation of less than 300 nm, but one also has to take the absorbance by SiO₂ into account (maximum about 250 nm)—therefore the chosen wavelength of 350–365 nm seems to be most suitable for the current system.

3. Results and discussion

3.1. General aspects

As pointed out before, one of the main difficulties with the incorporation of polymers into nanocomposites by the EISA method is preserving the order of the mesostructure in the various processing steps, in particular in the case of copolymers. Since the polymerization, especially of acrylates, can be strongly exothermic, the mesostructural order could become significantly distorted due to the fragility of the silica network at this stage and the temperature dependence of self-assembly. Fig. 2 shows XRD patterns acquired

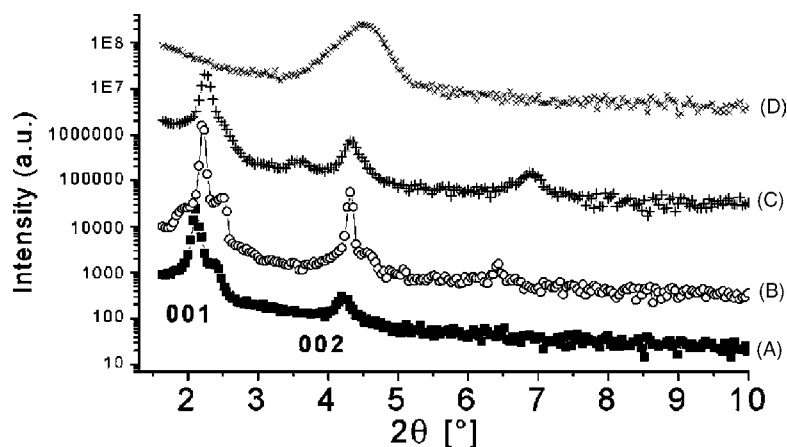


Fig. 2. X-ray diffraction patterns taken after the subsequent steps of the preparation of nanocomposites including polymers, using UV exposure: (■) as-prepared film; (○) film after UV exposure; (+) film after ammonia treatment; (×) films after washing with acetone.

from the same film at subsequent steps during the preparation, adding both dodecyl methacrylate and NIPAAM to the solution as monomers and using UV exposure. In this case, THF was added as solvent. The (00*l*) reflections are indicative of a lamellar mesostructure, with the lamellae being parallel to the substrate. For the as-prepared sample, the (001) reflection corresponds to a d-spacing of 4.2 nm, which represents the sum of the thickness of the silica layer and the organic layer. The sequence of XRD patterns shows that the polymerization in most cases does not lead to a substantial decrease in ordering, because the shape of the (00*l*) reflections does not change significantly. Only a small shift of the peak positions is observed towards larger values of 2θ (smaller d-spacing), which might be caused by the shrinkage of the silica network or the polymerization. However, washing the films with ethanol and acetone (to remove the surfactant and unreacted species) usually results in a decrease in ordering, as is seen by the broadening of the (001) reflection in Fig. 2. This might be a consequence of an inhomogeneous distribution of the polymer: assuming that the polymer chains are randomly distributed, domains are present with a difference in distance between the silica sheets. The decrease in d-spacing to approximately 2 nm is due to the removal of the surfactant and the resulting thinner organic layer. Spectroscopic ellipsometry was applied to determine the changes in the overall film thickness. While the thickness of a nanocomposite film was determined to be 800 ± 20 nm after thermal initiation, the same film had a thickness of ca. 400 ± 10 nm after surfactant removal. Taking into account that the lamellae are oriented parallel to the substrate, the 50% decrease in overall film thickness is in good compliance with the decrease in d-spacing from 4.2 to 2 nm.

In a series of experiments, the influence of various external parameters on the structure formation was studied. The following list includes some general observations:

1. Since the EISA method is governed by an evaporation process, the atmospheric humidity can affect the structure formation. No significant impact on the film quality and mesostructure was observed for relative humidities between 2 and 30%, while a relative humidity higher than 40% decreases the film stability.
2. The incorporation of a larger amount of polymer into the nanocomposite could theoretically be achieved by using higher concentrations of the monomer and the coupling agent (7-OTS). However, a massive decrease in film quality and also complete de-wetting of the films during dip-coating were observed when using higher concentrations than described in Section 2.
3. It appears that it is essential to filter the solution prior to dip- or spin-coating in order to get films of reasonable quality. So far, we can only speculate what moiety is removed by this procedure. Since aging of the solutions generally (after filtering) improves the film quality and the order of the mesostructure, condensed siliceous species or oligomers do not seem to be involved. Therefore, filtering might remove dust, but further investigations are needed to clarify this phenomenon.
4. The polarity of the solvent seems to be a relevant parameter; while the use of THF and ethanol leads to a reasonable film quality and well-defined mesostructure, no reasonable results were obtained with solvents of lower polarity, such as 1-butanol.

3.2. Coupling agents

3.2.1. Reactivity of the double bond

Because the coupling agents containing both an alkoxy group and a double bond are used as link between the polymer and the inorganic matrix, a certain reactivity of the molecule's double bond is essential. If the reactivity is too high, however, the coupling agent may already react before dip-coating or spin-coating, hence impairing the EISA process. Also, a too high reactivity might lead to a distortion of the mesostructure during the polymerization. Hence, optimum conditions have to be found balancing the favorable and damaging properties of the coupling agent. In this study, three different coupling agents were studied, trimethoxy(7-octen-1-yl)silane (7-OTS), 3-(trimethoxysilyl)propyl acrylate (PATMS) and 3-(trimethoxysilyl)propyl methacrylate (MPS). The reactivity of the double bond was studied by infrared spectroscopy and NMR for both UV- and thermally initiated polymerization. Since both techniques require larger amounts of materials than were obtainable from the thin films on silicon wafers, a different procedure was used to get sufficiently large quantities (Section 2). Both transmission electron microscopy and XRD revealed that this material shows a comparable ordering of the mesostructure. In addition, the reactivity of the double bond can be considered to be influenced by chemical parameters such as the initiator concentration and, in particular, the solvent, rather than the exact nature of the mesostructural environment.

Fig. 3 shows the IR spectra for films containing 7-OTS as coupling agent after UV exposure for various irradiation times. In a previous publication an irradiation time of 2 h was used [18]. The peak at approx. 1640 cm^{-1} is attributed to the 7-OTS double bond and shows a steady decrease over time. In order to get a semi-quantitative measure for the reactivity, the relative intensity was compared to the initiator peak at 1720 cm^{-1} . After 2 h of UV irradiation, the double bond peak still shows twice the intensity of the initiator peak. Even after 8 and 24 h, the peak is clearly visible; this proves a relatively low reactivity of the 7-OTS double bond upon irradiation with UV, which might be responsible for the limited reproducibility using UV exposure. Compared to 7-OTS, an acrylic or methacrylic double bond should show far greater reactivity. Additional experiments using a bulk solution of 7-OTS also revealed a moderate reactivity of the double bond under comparable conditions (initiator concentration, etc.). In order to find out if more reactive

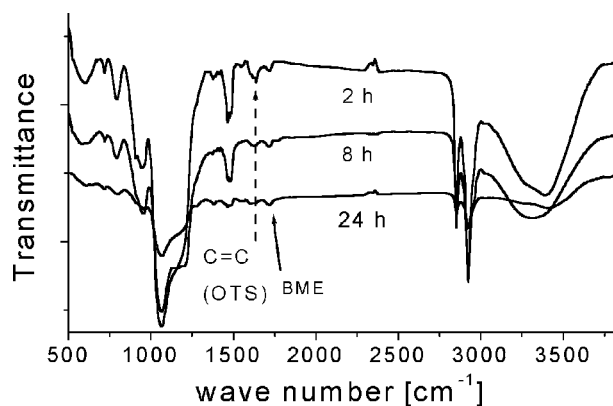


Fig. 3. IR spectra of OTS, embedded in a TEOS-based silica film, as a function of the UV exposure time. The arrows indicate the position of the double bond in OTS and BME residues (not assignable). The peak at 1500 cm^{-1} is due to the N-H groups in CTAB.

coupling agents are favorable for the preparation of polymer nanocomposite films, the reactivity of methacrylates was also studied by IR and NMR.

Fig. 4 illustrates a ^{13}C NMR study (direct polarization) of a film prepared from a solution containing PATMS, BME and A2**, before and after 2 h of UV irradiation. As the NMR pattern is quite complex due to the presence of several compounds with different chemical shifts, we will only focus on the peaks that are relevant in this context. The peaks at 166 and 130 ppm correspond to the carbonyl group and

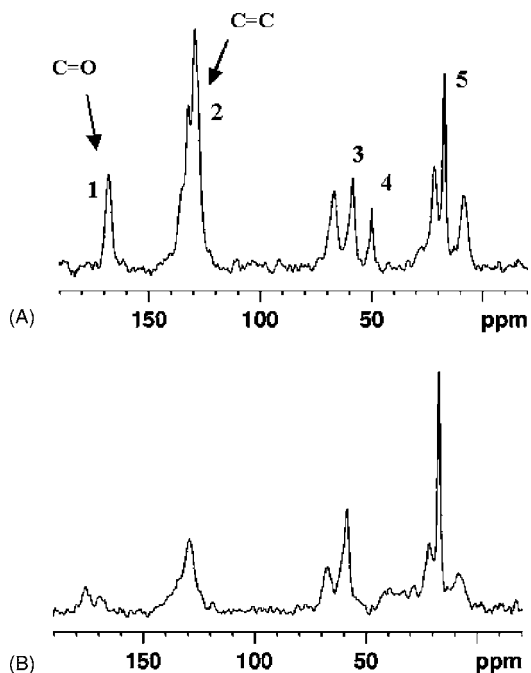


Fig. 4. ^{13}C NMR data of a film prepared with the PATMS coupling agent, before (A) and after (B) UV exposure for 2 h. Certain peaks could not be assigned unambiguously: 1, C=O group of the monomer (168 ppm, A and B) and the polymerized acrylate (175 ppm, B); 2, C=C double bond; 3 and 5, non-hydrolyzed ethoxy groups; 4, non-hydrolyzed methoxy groups.

the double bond of PATMS, respectively. In a separate experiment, it was found that the double bond peak at 130 ppm is convoluted by contributions from BME. Non-hydrolyzed ethoxy groups of A2** appear at 19 and 59 ppm, whilst the unreacted methoxy group of PATMS leads to the peak at 49 ppm. Due to the superposition of the PATMS double bond and BME at 130 ppm, the change in the chemical shift of the carbonyl group upon polymerization of the double bond was used to estimate the reactivity upon UV exposure. After UV exposure, the peak at 168 ppm is split up into two peaks corresponding to the initial unreacted PATMS and a new peak at 176 ppm corresponding to the carbonyl group of reacted PATMS. Integration indicates that approximately 62% of the PATMS double bonds reacted within the first 2 h of UV irradiation. Analogous NMR experiments with 7-OTS films reveal that only about 35% of the double bonds reacted under otherwise identical conditions. We therefore conclude that the reactivity of the double bond is significantly higher in PATMS and MPS compared to 7-OTS upon UV exposure. Similar experiments will elucidate the reactivity upon thermal initiation.

3.3. Influence of the coupling agent on the mesostructure

The results described in the previous section suggest that coupling agents with a highly reactive double bond are preferable for achieving a durable incorporation of polymers into the nanocomposite. However, certain problems emerged using PATMS and MPS as coupling agents; Fig. 5 shows XRD patterns obtained from a film after UV exposure and after ammonia treatment. It is observed that additional peaks are present at $2\theta = 3.5^\circ$ and $2\theta = 7^\circ$, which are attributed to CTAB crystallization. The presence of these CTAB peaks suggests that the lamellar mesostructure of the nanocomposite has been substantially disrupted by the CTAB crystals. Since this effect is only observed to this extent using PATMS and MPS as coupling agents, we speculate that the higher reactivity of the double bond leads to decreased mechanical stability of the mesostructure and/or surfactant phase separation.

3.4. Swelling experiments with poly(dodecyl methacrylate)/PNIPAAm copolymer-nanocomposites

In order to probe the thermoresponsiveness of the polymer-nanocomposite films, swelling experiments were performed using thermally polymerized washed samples with incorporated polymer. The swelling behavior was investigated by placing the samples in cold water (in a refrigerator, ca. 5°C), well below the lower critical solution temperature (LCST) of PNIPAAm (about 33°C). Deswelling was achieved analogously by immersing the wafers in water of 50°C . Fig. 6a shows the XRD spectrum of a film containing poly(dodecyl methacrylate), 7-OTS and the silica phase; these samples showed a only a low swelling and deswelling amplitude, which is apparent by a

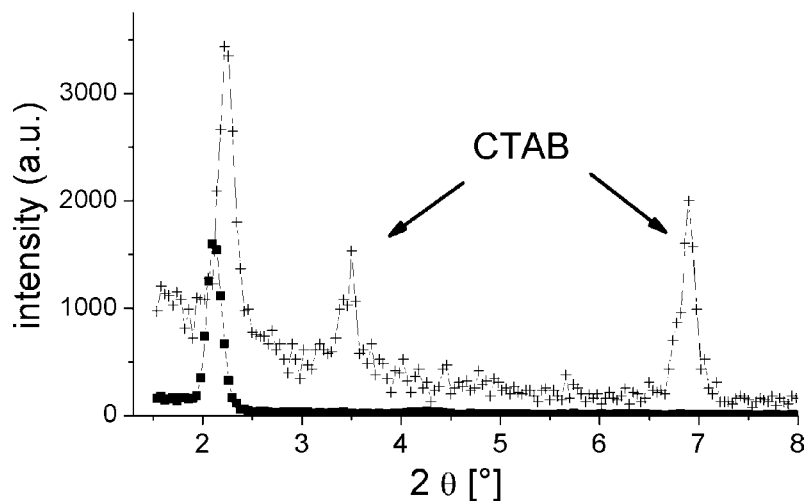


Fig. 5. XRD patterns of nanocomposite/polymer films using MPS as coupling agent: (■) film after UV exposure; (×) film after ammonia exposure (after UV exposure). In this case, crystallization of the surfactant (CTAB) occurs.

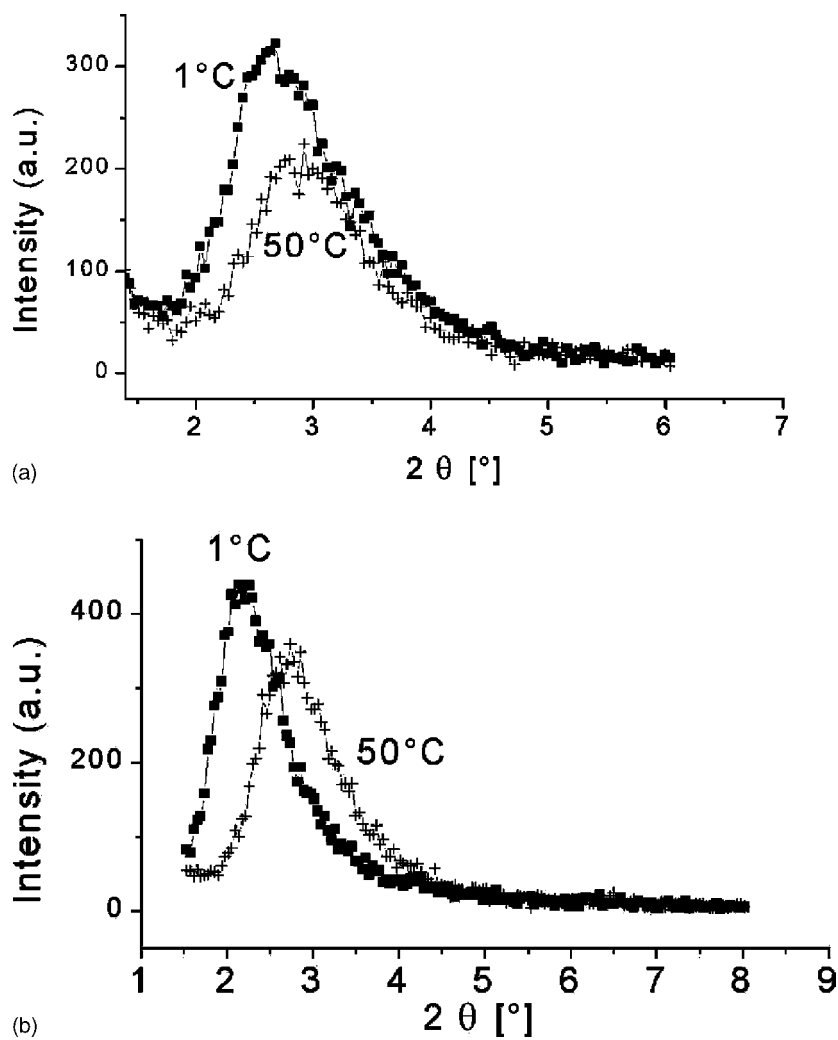


Fig. 6. XRD on the swelling behavior of nanocomposite films prepared with poly(dodecyl methacrylate) (a) and a copolymer of dodecyl methacrylate and NIPAAM (b).

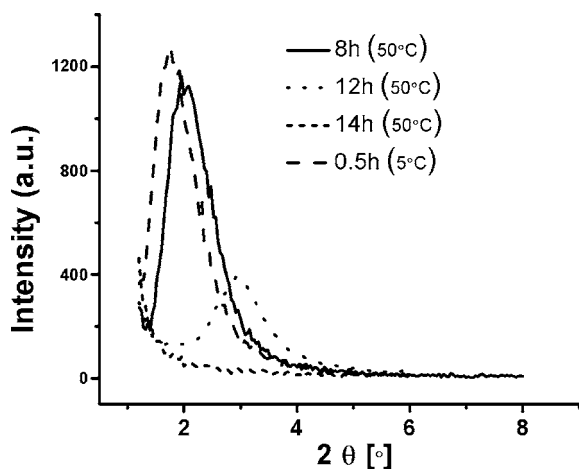


Fig. 7. XRD curves obtained from a film exposed to water at 50 °C as a function of time, followed by exposing the film to water of 5 °C for 0.5 h.

shift of the peak of $\Delta(2\theta) = 0.4^\circ$ at 1°C , corresponding to a change in d-spacing from 3.1 to 3.3 nm, which might be within the experimental error bar. In a similar experiment, PNIPAAm was added to the precursor solution. In this case, the degree of swelling is significantly higher, as illustrated in Fig. 6b: upon exposure to cold water, the (001) reflection shifted from an average d-spacing of 3.2–4.1 nm, and the amplitude of the deswelling in 50 °C water was similar. Also, our experiments show a tendency towards a faster swelling rate for the PNIPAAm system compared to the films only containing poly(dodecyl methacrylate) as polymer. So far, the swelling–deswelling behavior could not be observed by XRD over a larger number of cycles, which could be attributable to an XRD detectability effect rather than a dissolution/distortion of the film nanostructure. Fig. 7 shows XRD data of a film containing thermally polymerized poly(dodecyl methacrylate) and PNIPAAm, exposed to water of different temperature (5 and 50 °C). The XRD pattern of this film, immersed into water (50 °C) for 8 h, shows a pronounced (001) reflection at $2\theta = 2^\circ$, which was beyond the accessible range of our XRD instrument after treatment in water of 5 °C. This reflection peak is shifted to $2\theta = 3^\circ$ after further 2 h of exposure and shows a significant loss in scattering intensity. Further exposure for additional 2 h resulted in a complete disappearance of this reflection, although the film was measured under exactly identical conditions (position of sample holder in the XRD instrument). However, upon exposure to 5 °C water, the reflection peak reappeared at $2\theta = 1.6^\circ$ already after 30 min, also having the same shape as before this treatment. A longer exposure time in water of 5 °C results in a shift of the peak towards smaller scattering angles due to the swelling, causing the peak to completely disappear after 1 h. The remarkable scattering features of this film can be attributed to a quite pronounced and sensitive swelling behavior, also resulting in changes in the electron densities of the polymer layer. In general, the small-angle scattering

intensity $I(2\theta)$ of mesostructures, composed of two phases 1 and 2, is directly related to the average electron densities δ_1 and δ_2 of the two phases: $I(2\theta) \propto (\delta_1 - \delta_2)^2$. Therefore, the measurable XRD intensity of the lamellar mesostructure could eventually drop to an undetectable intensity due to changes in the average electron density of the polymer layer upon changes in the water content.

Our swelling experiments and the corresponding XRD experiments suggest that one major requirement is fulfilled using these polymers: in all cases the values of the d-spacing and the swelling behavior indicate that indeed monomer was incorporated and could be polymerized within the nanostructured environment. The significantly larger swelling amplitude for the poly(dodecyl methacrylate) + PNIPAAm system also suggests that a certain amount of PNIPAAm was incorporated, probably in the form of a copolymer with poly(dodecyl methacrylate), and also even exhibits its special thermoresponsive behavior in the confined environment of the nanocomposite films. Further experiments are needed to get unambiguous proof for the polymerization and incorporation of PNIPAAm, e.g. by DSC, TGA and NMR techniques. Also, detailed TGA studies will be performed to monitor the elution of polymer from the films upon exposure to water.

4. Conclusions

The scope of the present study is to find optimum conditions and parameters for the incorporation of water-based methacrylate polymers into lamellar organic/inorganic nanocomposite thin films. The influence of various parameters on the structure and chemical composition of the films was elucidated by XRD, NMR and IR techniques. Poly(dodecyl methacrylate) and its copolymers with poly(*N*-isopropylacrylamide) could be successfully incorporated into lamellar nanocomposite films by taking advantage of well-established techniques for the preparation of mesostructured thin films. In particular, it turned out that the mesostructure, induced by the recently introduced evaporation-induced self-assembly (EISA) technique, is not severely impeded by the presence of the polymers. Also, the nature of the coupling agent, which establishes a covalent linkage between the silica matrix and the polymer phase, has proved to be a crucial parameter: while trimethoxy(7-octen-1-yl) silane (7-OTS) shows a moderate reactivity of the double bond, the polymer/silica films were of reasonable quality with respect to the mesostructure and the swelling property of the polymers. In contrast, coupling agents containing more reactive acrylate double bonds massively distorted the film mesostructure. Future work has to elucidate the amount of polymer integrated in the mesostructure and will be dedicated to the incorporation of hydrogels into 3D mesostructured films. The hydrogel nanocomposite films could be of interest for a temperature or pH-controlled release of corrosion inhibitors.

Acknowledgements

This work was supported by Sandia National Laboratories, a Lockheed Martin Company, under Department of Energy Contract DE-AC04-94AL85000, the Air Force Office of Scientific Research Award Number F49620-01-1-0168, the DOE Office of Basic Energy Sciences (Division of Chemical Sciences, Geosciences, and Biosciences), the DOD MURI Program Contract 318651, and Sandia's Laboratory Directed Research and Development Program.

References

- [1] C. Kresge, M. Leonowicz, W. Roth, C. Vartuli, J. Beck, *Nature* 359 (1992) 710–714.
- [2] C.J. Brinker, Y.F. Lu, A. Sellinger, H.Y. Fan, *Adv. Mater.* 11 (1999) 579–585.
- [3] H. Yang, N. Coombs, I. Sokolov, G.A. Ozin, *Nature* 381 (1996) 589–592.
- [4] Y. Lu, R. Ganguli, C.A. Drewien, M.T. Anderson, C.J. Brinker, W. Gong, Y. Guo, H. Soyez, B. Dunn, M.H. Huang, J.I. Zink, *Nature* 389 (1997) 364–368.
- [5] C.J. Brinker, *Curr. Opin. Colloid Interface Sci.* 3 (1998) 166–173.
- [6] D. Grosso, A.R. Balkenende, P.A. Albouy, M. Lavergne, F. Babonneau, *J. Mater. Chem.* 10 (2000) 2085–2089.
- [7] D. Grosso, F. Babonneau, P.A. Albouy, H. Amenitsch, A.R. Balkenende, A. Brunet-Bruneau, J. Rivory, *Chem. Mater.* 2 (2002) 931–939.
- [8] S. Besson, T. Gacoin, C. Jacquot, C. Ricolleau, D. Babonneau, J.-P. Boilot, *J. Mater. Chem.* 10 (2000) 1331–1337.
- [9] D. Grosso, A.R. Balkenende, P.A. Albouy, A. Ayrat, H. Amenitsch, F. Babonneau, *Chem. Mater.* 13 (2001) 1848–1856.
- [10] D. Grosso, F. Babonneau, G.J.A.A. de Soler-Illia, P.A. Albouy, H. Amenitsch, *Chem. Commun.* (2002) 748–749.
- [11] M. Klotz, P.A. Albouy, A. Ayrat, C. Ménager, D. Grosso, A. Van der Lee, V. Cabuil, C. Guizard, *Chem. Mater.* 12 (2000) 1721–1728.
- [12] R.D. Miller, *Science* 286 (1999) 421–423.
- [13] R.A. Caruso, A. Susha, F. Caruso, *Chem. Mater.* 13 (2001) 400–409.
- [14] F. Hua, Y. Lvov, T.H. Cui, *J. Nanosci. Nanotechnol.* 2 (2002) 357–361.
- [15] O. Soppera, C. Croutxe-Barghorn, C. Carre, D. Blanc, *Appl. Surf. Sci.* 186 (2002) 91–94.
- [16] Y. Lee, J. Kim, Y. Son, *Polymer-Korea* 23 (1999) 443–449.
- [17] Y. Lu, H. Fan, N. Doke, D.A. Loy, R.A. Assink, D.A. LaVan, C.J. Brinker, *J. Am. Chem. Soc.* 122 (2000) 5258–5261.
- [18] A. Sellinger, P.M. Weiss, A. Nguyen, Y. Lu, R.A. Assink, W. Gong, C.J. Brinker, *Nature* 394 (1998) 256–260.
- [19] Y. Lu, Y. Yang, A. Sellinger, M. Lu, J. Huang, H. Fan, R. Haddad, G. Lopez, A.R. Burns, D.Y. Sasaki, J. Shelnett, C.J. Brinker, *Nature* 410 (2001) 913–917.
- [20] E. Diez-Pena, I. Quijada-Garrido, P. Frutos, J.M. Barrales-Rienda, *Macromolecules* 35 (2002) 2667–2675.
- [21] F.M. Winnik, *Polymer* 31 (1990) 2125–2134.
- [22] H.G. Schild, *Prog. Polym. Sci.* 17 (1992) 163–249.
- [23] L. Liang, J. Liu, X. Gong, *Langmuir* 16 (2000) 9895–9899.